Towards first-principles understanding of the metal–insulator transition in fluid alkali metals



2009 J. Phys.: Condens. Matter 21 064205

(http://iopscience.iop.org/0953-8984/21/6/064205)

J. Phys.: Condens. Matter **21** (2009) 064205 (6pp) doi:10.1088/0953-8984/21/6/064205

# Towards first-principles understanding of the metal–insulator transition in fluid alkali metals

**H Maebashi and Y Takada**

Institute for Solid State Physics, University of Tokyo, Kashiwa, Chiba 277-8581, Japan

E-mail: maebashi@issp.u-tokyo.ac.jp

Received 27 June 2008
Published 20 January 2009
Online at stacks.iop.org/JPhysCM/21/064205

**Abstract**

By treating the electron–ion interaction as a perturbation in the first-principles Hamiltonian, we have calculated the density response functions of a fluid alkali metal to find an interesting charge instability due to anomalous electronic density fluctuations occurring at some finite wavevector $\boldsymbol{Q}$ in a dilute fluid phase above the liquid–gas critical point. Since $|\boldsymbol{Q}|$ is smaller than the diameter of the Fermi surface, this instability necessarily impedes the electric conduction, implying its close relevance to the metal–insulator transition in fluid alkali metals.

(Some figures in this article are in colour only in the electronic version)

## 1. Introduction

The metal–insulator transition in fluid alkali metals such as Rb and Cs has long been attracting attention [1, 2], partly because this might be a faithful manifestation of the 'Mott transition' in its original sense [3] or the one driven by an insufficiently screened Coulomb potential and partly because this accompanies the liquid–gas phase transition, the same situation as first considered in mercury by Landau and Zeldovich [4].

In the density–temperature phase diagram of the alkali metals, the liquid-phase region is bounded above by the critical point and below by the triple point, as in the systems of rare-gas atoms [5]. Above the critical point, there exists the fluid-phase region, an interesting phase in which the metal–insulator transition occurs. In many respects, the properties of the dense supercritical fluid are not very different from those of the liquid and a well known charge instability develops near the transition from liquid to solid, as the electronic (ionic) density, $n$, increases or as the Wigner–Seitz radius of electrons (ions) in atomic units, $r_s$, decreases. We can expect, however, to observe a different type of charge instability closely related to the metal–insulator transition as $r_s$ increases in the fluid phase.

Conventionally, liquid alkali metals are studied by treating the bare electron–ion (pseudo)potential as a perturbation to provide an effective ion–ion interaction via the sea of valence electrons described by the three-dimensional electron gas (3DEG) [6]. The exchange–correlation effects of the valence electrons play an important role in the dilute fluid with large $r_s$. It is fortunate that in developing the first-principles calculation based on the density functional theory useful information on the 3DEG is now available in a wide range of $r_s$. In this paper, we investigate the density response of the fluid alkali metal to find the charge instability for low densities by use of the standard perturbation approach, together with this information on 3DEG. Throughout this paper, we employ atomic units.

## 2. Response functions in the first-principles Hamiltonian

The alkali metals composed of $N$ electrons and $N$ ions are well described by the following Hamiltonian:

$$H = T_{\mathrm{e}} + T_{\mathrm{i}} + U_{\mathrm{ee}} + U_{\mathrm{ii}} + U_{\mathrm{ei}}, \tag{1}$$

with

$$T_{\mathrm{e}} = \sum_{j=1}^{N} \frac{\boldsymbol{p}_j^2}{2m}, \qquad T_{\mathrm{i}} = \sum_{j=1}^{N} \frac{\boldsymbol{P}_j^2}{2M},$$

$$U_{\mathrm{ee}} = \frac{1}{2} \sum_{j \neq j'} V_{\mathrm{ee}}(\boldsymbol{r}_j - \boldsymbol{r}_{j'}), \qquad U_{\mathrm{ii}} = \frac{1}{2} \sum_{j \neq j'} V_{\mathrm{ii}}(\boldsymbol{R}_j - \boldsymbol{R}_{j'}),$$

$$U_{\mathrm{ei}} = \sum_{j,j'} V_{\mathrm{ei}}(\boldsymbol{r}_j - \boldsymbol{R}_{j'}), \tag{2}$$

 

where $\{\boldsymbol{r}_j\}$ and $\{\boldsymbol{R}_j\}$ denote, respectively, electronic and ionic coordinates, $\{\boldsymbol{p}_j\}$ and $\{\boldsymbol{P}_j\}$ corresponding momenta, $m$ and $M$ the masses and $V_{\rm ee}(\boldsymbol{r})$, $V_{\rm ii}(\boldsymbol{R})$ and $V_{\rm ei}(\boldsymbol{r})$ the bare electron–electron, ion–ion and electron–ion interactions. At long distances $V_{\rm ii}(\boldsymbol{R})$ as well as $V_{\rm ei}(\boldsymbol{r})$ is represented by a purely Coulombic form, but it deviates from it at short-range distances due to the van der Waals attraction and the Born–Mayer repulsion between ionic cores for $V_{\rm ii}(\boldsymbol{R})$ or due to orthogonality between the valence- and core-electron wavefunctions for $V_{\rm ei}(\boldsymbol{r})$; the former contribution is weak for alkali metals and the latter can be well captured by adopting a suitable (local) pseudopotential $V_{\rm ei}(\boldsymbol{r}) = V_{\rm ps}(\boldsymbol{r})$. In general, the Fourier transforms of these interactions $V_{\alpha\beta}(\boldsymbol{q})$ can be written in terms of an effective valence, $Z_\alpha(\boldsymbol{q})$, characterizing the long-range Coulomb interaction and a short-range part, $U_{\alpha\beta}(\boldsymbol{q})$, as

$$V_{\alpha\beta}(\boldsymbol{q}) = Z_\alpha(\boldsymbol{q})Z_\beta(\boldsymbol{q})v(\boldsymbol{q}) + U_{\alpha\beta}(\boldsymbol{q}), \tag{3}$$

where $\alpha$ and $\beta$ denote species of the particles, e (electron) or i (ion). Here $Z_{\rm e}(\boldsymbol{q}) = -1$, $Z_{\rm i}(\boldsymbol{q}) = |V_{\rm ps}(\boldsymbol{q})|/v(\boldsymbol{q})$, $U_{\alpha\beta}(\boldsymbol{q}) = 0$ unless $\alpha = \beta = {\rm i}$, and $U_{\rm ii}(\boldsymbol{q})$ represents the short-range interaction between ionic cores. Reflecting the purely Coulombic nature of both $V_{\rm ii}(\boldsymbol{R})$ and $V_{\rm ei}(\boldsymbol{r})$ at long distances, $Z_{\rm i}(\boldsymbol{q}) \to 1$ and $U_{\rm ii}(\boldsymbol{q})$ converges to a finite value in the limit of $q \equiv |\boldsymbol{q}| \to 0$.

Since the first term in the right-hand side of (3) is proportional to $v(\boldsymbol{q}) = 4\pi/q^2$ and gets singular at $q \to 0$, it is useful to write the partial number-density response function $\chi_{\alpha\beta}(\boldsymbol{q},\omega)$ in terms of its proper part $\Pi_{\alpha\beta}(\boldsymbol{q},\omega)$, which is irreducible with respect to $v(\boldsymbol{q})$ but not to $U_{\alpha\beta}(\boldsymbol{q})$, as

$$\chi_{\alpha\beta}(\boldsymbol{q},\omega) = -\Pi_{\alpha\beta}(\boldsymbol{q},\omega) - v(\boldsymbol{q}) \sum_{\gamma,\delta={\rm e,i}} \Pi_{\alpha\gamma}(\boldsymbol{q},\omega)Z_\gamma(\boldsymbol{q})Z_\delta(\boldsymbol{q})\chi_{\delta\beta}(\boldsymbol{q},\omega), \tag{4}$$

which is rewritten as

$$\chi_{\alpha\beta}(\boldsymbol{q},\omega) = -\Pi_{\alpha\beta}(\boldsymbol{q},\omega) + v(\boldsymbol{q}) \sum_{\gamma,\delta={\rm e,i}} \frac{\Pi_{\alpha\gamma}(\boldsymbol{q},\omega)Z_\gamma(\boldsymbol{q})Z_\delta(\boldsymbol{q})\Pi_{\delta\beta}(\boldsymbol{q},\omega)}{1 + v(\boldsymbol{q})\Pi_{ZZ}(\boldsymbol{q},\omega)}, \tag{5}$$

where the polarization function is defined as $\Pi_{ZZ}(\boldsymbol{q},\omega) \equiv \sum_{\alpha\beta} Z_\alpha(\boldsymbol{q})Z_\beta(\boldsymbol{q})\Pi_{\alpha\beta}(\boldsymbol{q},\omega)$. In the two-component Coulomb system with the effective valences $Z_\alpha(\boldsymbol{q})$, the charge density is given by the sum of ionic and electronic valence densities, while the (total) number density by the sum of ionic and electronic number densities. Then, by use of (5), the charge-density response function $\chi_{ZZ}(\boldsymbol{q},\omega) \equiv \sum_{\alpha\beta} Z_\alpha(\boldsymbol{q})Z_\beta(\boldsymbol{q})\chi_{\alpha\beta}(\boldsymbol{q},\omega)$, the number-density response function $\chi_{NN}(\boldsymbol{q},\omega) \equiv \sum_{\alpha\beta} \chi_{\alpha\beta}(\boldsymbol{q},\omega)$, and the cross response function $\chi_{NZ}(\boldsymbol{q},\omega) \equiv \sum_{\alpha\beta} Z_\beta(\boldsymbol{q})\chi_{\alpha\beta}(\boldsymbol{q},\omega)$ are, respectively, obtained as

$$\chi_{ZZ}(\boldsymbol{q},\omega) = -\frac{\Pi_{ZZ}(\boldsymbol{q},\omega)}{1 + v(\boldsymbol{q})\Pi_{ZZ}(\boldsymbol{q},\omega)}, \tag{6}$$

$$\chi_{NN}(\boldsymbol{q},\omega) = -\Pi_{NN}(\boldsymbol{q},\omega) + \frac{v(\boldsymbol{q})\Pi_{NZ}(\boldsymbol{q},\omega)\Pi_{ZN}(\boldsymbol{q},\omega)}{1 + v(\boldsymbol{q})\Pi_{ZZ}(\boldsymbol{q},\omega)}, \tag{7}$$

$$\chi_{NZ}(\boldsymbol{q},\omega) = -\frac{\Pi_{NZ}(\boldsymbol{q},\omega)}{1 + v(\boldsymbol{q})\Pi_{ZZ}(\boldsymbol{q},\omega)}, \tag{8}$$

where $\Pi_{NN}(\boldsymbol{q},\omega) = \sum_{\alpha\beta} \Pi_{\alpha\beta}(\boldsymbol{q},\omega)$, $\Pi_{NZ}(\boldsymbol{q},\omega) = \sum_{\alpha\beta} Z_\beta(\boldsymbol{q})\Pi_{\alpha\beta}(\boldsymbol{q},\omega)$, and $\Pi_{ZN}(\boldsymbol{q},\omega) = \sum_{\alpha\beta} Z_\alpha(\boldsymbol{q})\Pi_{\alpha\beta}(\boldsymbol{q},\omega)$.

Some comments are in order for the so-called $q$-limits of these response functions. In 3DEG or an unperturbed electron system for (1), the charge neutrality condition and the compressibility sum rule lead, respectively, to the relations $\lim_{q\to0} \chi^{(0)}_{\rm ee}(\boldsymbol{q},0) = 0$ and $\lim_{q\to0} \Pi^{(0)}_{\rm ee}(\boldsymbol{q},0) = n^2\kappa$ with the superscript (0) implying 'unperturbed' with respect to $U_{\rm ei}$, where $\kappa$ is the compressibility of the 3DEG. These relations reflect a special feature of a single-component Coulomb system with a rigid compensated-charge background such as the 3DEG in which we cannot distinguish the charge-density response function from the number-density one. In the two-component Coulomb system, on the other hand, there is a difference between them and the difference leads to important modifications on these relations. More specifically, the charge neutrality condition leads to

$$\lim_{q\to0} \chi_{ZZ}(\boldsymbol{q},0) = \lim_{q\to0} \chi_{NZ}(\boldsymbol{q},0) = 0, \tag{9}$$

while the compressibility sum rule relates the $q$-limit of $\chi_{NN}(\boldsymbol{q},\omega)$ to the isothermal compressibility $K_T$ of the total electron–ion system. Then, from (5) and (7), it is not hard to see that $\chi_{\alpha\beta}(\boldsymbol{q},\omega)$ satisfies the following relations for arbitrary $\alpha$ and $\beta$ [7]:

$$\lim_{q\to0} \chi_{\alpha\beta}(\boldsymbol{q},0) = \tfrac{1}{4} \lim_{q\to0} \chi_{NN}(\boldsymbol{q},0) = -n^2K_T. \tag{10}$$

Note that the $q$-limit of $\chi_{\rm ee}(\boldsymbol{q},\omega)$ does not vanish but takes a finite value $-n^2K_T$, although $\lim_{q\to0} \chi^{(0)}_{\rm ee}(\boldsymbol{q},0) = 0$. By (10), we can identify the liquid–gas phase transition from a singularity in $\chi_{\alpha\beta}(\boldsymbol{q},0)$, particularly in the ionic number-density response function $\chi_{\rm ii}(\boldsymbol{q},0)$ at $q = 0$, because $K_T$ diverges at the critical point. Note also that by (9) the singularity implying a charge instability can occur only at a *finite* $q$.

## 3. Approximate response functions based on effective ion–ion interaction

Following Ashcroft and Stroud [6], we can derive an effective ionic Hamiltonian $\tilde{H}_{\rm i} = T_{\rm i} + \tilde{U}_{\rm ii} + N\tilde{u}_0$ by applying a perturbative method with respect to $U_{\rm ei}$ in (1), where $\tilde{u}_0$ is an energy shift independent of $\{\boldsymbol{P}_j\}$ and $\{\boldsymbol{R}_j\}$ (but dependent on $n$). The interaction term $\tilde{U}_{\rm ii}$ can be described by a pairwise sum of effective ion–ion interactions as

$$\tilde{U}_{\rm ii} = \tfrac{1}{2} \sum_{j\neq j'} \tilde{V}_{\rm ii}(\mathbf{R}_j - \mathbf{R}_{j'}). \tag{11}$$

Here the Fourier transform of the effective ion–ion interaction $\tilde{V}_{\rm ii}(\mathbf{R})$ is given by

$$\tilde{V}_{\rm ii}(\boldsymbol{q}) = Z_{\rm i}(\boldsymbol{q})^2 v(\boldsymbol{q})/\varepsilon(\boldsymbol{q}) + U_{\rm ii}(\boldsymbol{q}), \tag{12}$$

with $\varepsilon(\boldsymbol{q})$ the static dielectric function of 3DEG defined as

$$\varepsilon(\boldsymbol{q}) = 1 + v(\boldsymbol{q})\Pi^{(0)}_{\rm ee}(\boldsymbol{q},0). \tag{13}$$

Equation (12) indicates that the long-range part of the bare ion–ion interaction $V_{ii}(q)$, the first term in the right-hand side of (3), has been screened by the surrounding valence electrons, while the short-range part $U_{ii}(q)$ remains intact.

We shall calculate the ionic structure factor $S_{ii}(q)$ in this electron–ion system by using the effective ionic Hamiltonian. Since ions can be considered as classical particles, the classical version of the fluctuation-dissipation theorem relates $S_{ii}(q)$ to the static response function $\chi_{ii}(q, 0)$ as

$$\chi_{ii}(q, 0) = -nS_{ii}(q)/T. \tag{14}$$

In the same spirit as in (4), we shall introduce $\Pi_{ii}(q, 0)$, the proper part irreducible with respect to $v(q)$, to write $\chi_{ii}(q, 0)$ as

$$\begin{aligned}\chi_{ii}(q, 0) &= -[\Pi_{ii}(q, 0)^{-1} + Z_i(q)^2 v(q)/\varepsilon(q)]^{-1} \\ &= -\Pi_{ii}(q, 0) + \frac{v(q)Z_i(q)^2\Pi_{ii}(q, 0)^2}{1 + v(q)[\Pi^{(0)}_{ee}(q, 0) + Z_i(q)^2\Pi_{ii}(q, 0)]}.\end{aligned} \tag{15}$$

By comparing (15) with (5), we find that $\Pi_{ee}(q, 0) = \Pi^{(0)}_{ee}(q, 0)$ and $\Pi_{ei}(q, 0) = \Pi_{ie}(q, 0) = 0$ at least in the present approximation. Substituting these equations and (14) into (5), we obtain

$$\begin{aligned}\chi_{ee}(q, 0) = &-\frac{1}{v(q)}\left(1 - \frac{1}{\varepsilon(q)}\right) \\ &- Z_i(q)^2\left(1 - \frac{1}{\varepsilon(q)}\right)^2 nS_{ii}(q)/T,\end{aligned} \tag{16}$$

$$\chi_{ei}(q, 0) = \chi_{ie}(q, 0) = -Z_i(q)\left(1 - \frac{1}{\varepsilon(q)}\right) nS_{ii}(q)/T. \tag{17}$$

From (14), (16) and (17), the static charge-density, number-density and cross response functions are, respectively, given by

$$\begin{aligned}\chi_{ZZ}(q, 0) = &-\frac{1}{v(q)}\left(1 - \frac{1}{\varepsilon(q)}\right) \\ &- \frac{Z_i(q)^2}{\varepsilon(q)^2} nS_{ii}(q)/T,\end{aligned} \tag{18}$$

$$\begin{aligned}\chi_{NN}(q, 0) = &-\frac{1}{v(q)}\left(1 - \frac{1}{\varepsilon(q)}\right) \\ &- \left(1 + Z_i(q) - \frac{Z_i(q)}{\varepsilon(q)}\right)^2 nS_{ii}(q)/T,\end{aligned} \tag{19}$$

$$\begin{aligned}\chi_{NZ}(q, 0) = &\frac{1}{v(q)}\left(1 - \frac{1}{\varepsilon(q)}\right) \\ &- \frac{Z_i(q)}{\varepsilon(q)}\left(1 + Z_i(q) - \frac{Z_i(q)}{\varepsilon(q)}\right) nS_{ii}(q)/T.\end{aligned} \tag{20}$$

We can easily check that these response functions satisfy the required conditions of (9) and (10) with $\lim_{q\to 0}\chi_{ii}(q, 0) = -nS_{ii}(\mathbf{0})/T = -n^2K_T$.

In what follows, for simplicity, we take $V_{ii}(\boldsymbol{R}) = |\boldsymbol{R}|^{-1}$ and $V_{ei}(\boldsymbol{r}) = V^{(A)}_{ps}(\boldsymbol{r})$, where $V^{(A)}_{ps}(\boldsymbol{r})$ is the Ashcroft's empty-core pseudopotential, given by

$$V^{(A)}_{ps}(\boldsymbol{r}) = \begin{cases} 0 & |\boldsymbol{r}| < r_c \\ -|\boldsymbol{r}|^{-1} & |\boldsymbol{r}| > r_c \end{cases} \tag{21}$$

with $r_c$ being the radius of the ionic core; this simplification leads to $Z_i(q) = \cos(qr_c)$ and $U_{ii}(q) = 4\pi[1-\cos^2(qr_c)]/q^2$. For $\varepsilon(q)$, we use an accurate parametrization of the diffusion Monte Carlo data of the 3DEG at $T = 0$ by Moroni *et al* [8].

## 4. Comparison of mean-field approximation with Monte Carlo simulation

We shall now solve the effective ionic Hamiltonian to obtain $S_{ii}(q)$ in the mean-field approximation, one of the standard methods in the theory of simple liquids, together with Monte Carlo simulations.

Suppose that the effective ion–ion interaction, $\tilde{V}_{ii}(\boldsymbol{R}) = (2\pi^2 R)^{-1}\int_0^\infty \mathrm{d}q\,\tilde{V}_{ii}(q)q\sin(qR)$ with $R \equiv |\mathbf{R}|$, can be expressed as the sum of a 'reference' part, $v_0(\boldsymbol{R})$, and a 'perturbation', $w(\boldsymbol{R})$, by

$$\tilde{V}_{ii}(\boldsymbol{R}) = v_0(\boldsymbol{R}) + w(\boldsymbol{R}). \tag{22}$$

In the mean-field approximation, the free-energy functional $F[n_i]$ of the ionic number density $n_i(\boldsymbol{R})$ for the system of interest, characterized by the full potential $\tilde{V}_{ii}(\boldsymbol{R})$, is simply related to that of the reference system $F_0[n_i]$ by

$$F[n_i] = F_0[n_i] + \tfrac{1}{2}\int\int n_i(\boldsymbol{R})w(\boldsymbol{R} - \boldsymbol{R}')n_i(\boldsymbol{R}')\,\mathrm{d}\boldsymbol{R}\,\mathrm{d}\boldsymbol{R}'. \tag{23}$$

Then, we can expand the thermodynamic potential $\Omega[n_i] = F[n_i] - \mu_i\int n_i(\boldsymbol{R})\,\mathrm{d}\boldsymbol{R}$ (with $\mu_i$ being the chemical potential of ions) up to second order with respect to the ionic number-density fluctuations $n_i(q)$ as

$$\Omega[n_i] = \Omega(n) + \frac{T}{2n}\sum_{q\neq\mathbf{0}} S_{ii}(q)^{-1}n_i(q)n_i(-q) + \cdots. \tag{24}$$

Here $S_{ii}(q)$ is the ionic structure factor in the mean-field approximation, given by

$$S_{ii}(q) = [S_0(q)^{-1} + nw(q)/T]^{-1}, \tag{25}$$

where $S_0(q)$ is the structure factor of the reference system and $w(q)$ is the Fourier transform of $w(\boldsymbol{R})$.

The result of the present mean-field approximation depends on how to separate the interaction into a reference part $v_0(\boldsymbol{R})$ and a perturbation $w(\boldsymbol{R})$. A number of separations have been proposed so far for the Lennard-Jones potential; among them, here we adopt the manner of Weeks, Chandler and Andersen, usually called the WCA separation [9]. In this separation, as shown in figure 1, the interaction is split at $R = R_0$, the position of the minimum of $\tilde{V}_{ii}(\boldsymbol{R})$, into its purely repulsive and almost attractive parts; $v_0(\boldsymbol{R}) = \tilde{V}_{ii}(\boldsymbol{R}) - E_0$ and $w(\boldsymbol{R}) = E_0$ for $R < R_0$, while $v_0(\boldsymbol{R}) = 0$ and $w(\boldsymbol{R}) = \tilde{V}_{ii}(\boldsymbol{R})$ for $R > R_0$, where $E_0$ is the minimum value of $\tilde{V}_{ii}(\boldsymbol{R})$ at $R = R_0$. The reference system with the purely repulsive interaction $v_0(\boldsymbol{R})$ can be effectively treated as a hard-sphere fluid where the diameter of the hard sphere is defined as

$$d = \int_0^\infty (1 - \mathrm{e}^{-v_0(R)/T})\,\mathrm{d}R. \tag{26}$$

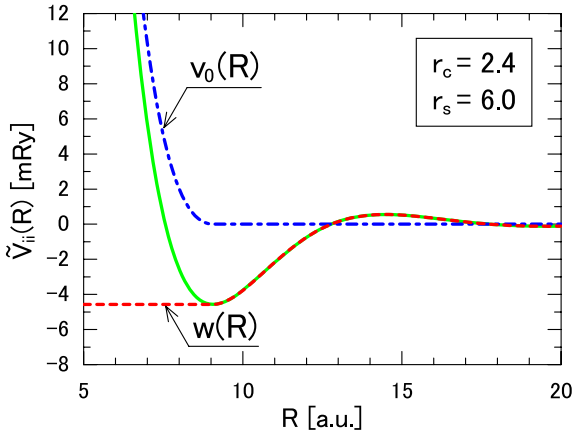


**Figure 1.** Effective ion–ion interaction $\tilde{V}_{ii}(\boldsymbol{R})$ for $r_s = 6.0$ and $r_c = 2.4$ (the solid curve), which is divided into the reference part, $v_0(\boldsymbol{q})$ (the chain curve), and the perturbation, $w(\boldsymbol{q})$ (the broken curve), in the WCA separation.

Using the analytic solution of the Percus–Yevick equation for this hard-sphere fluid [10–12], we can obtain $S_0(\boldsymbol{q})$ and therefore $S_{ii}(\boldsymbol{q})$ by (25).

Figure 2 shows the ionic structure factor $S_{ii}(\boldsymbol{q})$ calculated in this mean-field approximation based on the WCA separation (the broken curves) and by Monte Carlo simulations (the solid curves) for temperatures and densities corresponding to the conditions of the recent experiments for a liquid Rb [13]. Note that for all the values of $T$ and $r_s$ in figure 2 the Monte Carlo results are in good accord with the experimental data, which has not been shown here. Although the quantitative disagreement between mean-field and Monte Carlo results can be observed in the vicinity of the triple point (e.g. $T = 373$ K, $r_s = 5.39$) and in the vicinity of the critical point (e.g. $T = 2173$ K, $r_s = 7.56$), we can find that the mean-field approximation reproduces at least qualitative features of the Monte Carlo results for $S_{ii}(\boldsymbol{q})$ such as the peak position. In the next section, with this knowledge of the mean-field approximation, we will investigate the charge-density response of the system in a fluid phase above the critical point.

## 5. Charge instability in a fluid phase above the critical point

As discussed in section 2, a charge instability is signaled by a divergence in $\chi_{ii}(\boldsymbol{q}, 0) = -nS_{ii}(\boldsymbol{q})/T$ at $q = Q \equiv |\boldsymbol{Q}|$ with $\boldsymbol{Q}$ being a certain *finite* wavevector, while the compressible instability by that at $q = 0$. In fact, the mean-field approximation based on the WCA separation leads us to the result that $S_{ii}(\boldsymbol{q})$ diverges for low densities as shown in figure 3, from which the divergence is seen to occur at $q = Q \sim 0.2$ for $r_s = 14$ (the broken curve) and $r_s = 16$ (the chain curve), but at $q = 0$ for $r_s = 12.3$ (the solid curve). Figure 4 presents the 'phase diagram' in the $r_s$–$T$ plane in which the charge instability occurs along the solid curve, while the compressible instability along the broken curve, the former preceding the latter with decreasing temperature in the shaded region of $r_s > 12.3$.

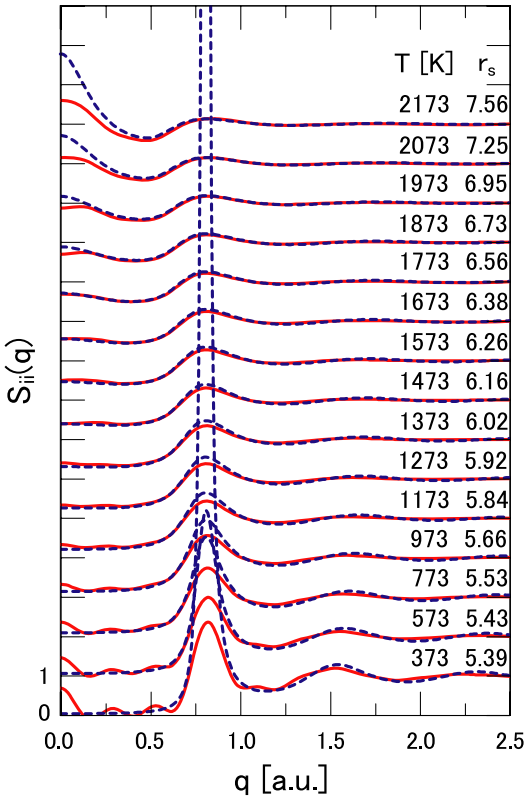


**Figure 2.** Ionic structure factor $S_{ii}(\boldsymbol{q})$ in a liquid phase of Rb ($r_c = 2.4$). The solid and broken curves represent Monte Carlo and mean-field results, respectively.

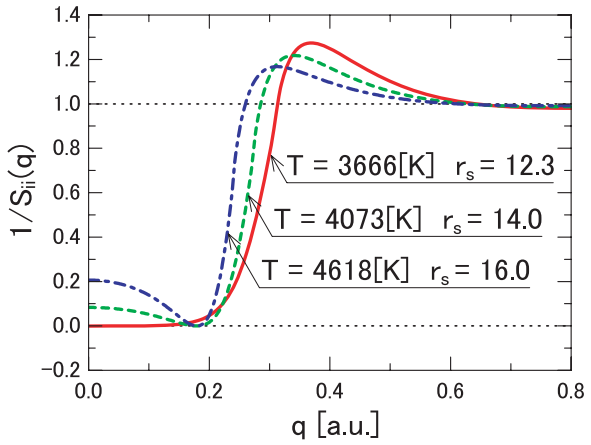


**Figure 3.** Inverse of the ionic structure factor $S_{ii}(\boldsymbol{q})$ in the mean-field approximation based on the WCA separation for low densities of $r_s = 12.3$, 14.0 and 16.0 with the core radius of $r_c = 2.4$.

To obtain a deeper insight into this charge instability in the dilute fluid phase of $r_s > 12.3$, let us consider the charge-density modulation induced by a negative point charge put into the origin of the system. This charge-density modulation is given by $\delta\rho(\boldsymbol{q}) = -\chi_{ZZ}(\boldsymbol{q}, 0)v(\boldsymbol{q})$ in the linear response theory, which is a total of $\delta\rho_e(\boldsymbol{q}) = -Z_e(\boldsymbol{q})\sum_\alpha \chi_{e\alpha}(\boldsymbol{q}, 0)Z_\alpha(\boldsymbol{q})v(\boldsymbol{q})$ and $\delta\rho_i(\boldsymbol{q}) = -Z_i(\boldsymbol{q})\sum_\alpha \chi_{i\alpha}(\boldsymbol{q}, 0)Z_\alpha(\boldsymbol{q})v(\boldsymbol{q})$ with $\delta\rho_e(\boldsymbol{q})$ and $\delta\rho_i(\boldsymbol{q})$ being electronic and ionic induced charges, respectively.

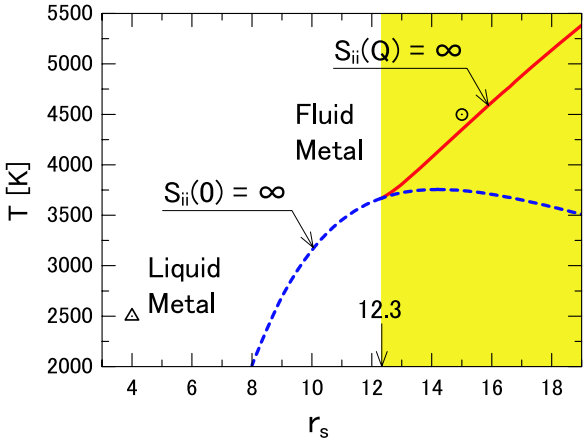


**Figure 4.** Charge and compressible instabilities in the mean-field approximation based on the WCA separation for $r_c = 2.4$. The structure factor $S_{ii}(\boldsymbol{q})$ diverges at $\boldsymbol{q} = \boldsymbol{Q}$ (with $\boldsymbol{Q}$ being a certain finite momentum) along the solid curve, while at $\boldsymbol{q} = \boldsymbol{0}$ along the broken curve in the $r_s$–$T$ plane.

From (14), (16) and (17), we can write down

$$\delta\rho_e(\boldsymbol{q}) = \left(1 - \frac{1}{\varepsilon(\boldsymbol{q})}\right)\left(1 - \frac{Z_i(\boldsymbol{q})^2 v(\boldsymbol{q})}{\varepsilon(\boldsymbol{q})} n S_{ii}(\boldsymbol{q})/T\right), \quad (27)$$

$$\delta\rho_i(\boldsymbol{q}) = \frac{Z_i(\boldsymbol{q})^2 v(\boldsymbol{q})}{\varepsilon(\boldsymbol{q})} n S_{ii}(\boldsymbol{q})/T. \quad (28)$$

Figure 5 presents $\delta\rho_e(\boldsymbol{q})$ (the broken curve), $\delta\rho_i(\boldsymbol{q})$ (the chain curve) and $\delta\rho(\boldsymbol{q})$ (the solid curve) at two typical points in the $r_s$–$T$ plane marked by (a) the circle with a dot and (b) the triangle with a dot in figure 4; we are interested in the charge-density modulations for low densities in the former, but for comparison we also show those for high densities in the latter, which indicate a well known charge instability related to the transition from liquid to solid. In both cases (a) and (b), the charge neutrality condition $\delta\rho(\boldsymbol{0}) = 1$ is satisfied by the fact that the external point charge is completely screened by the electrons ($|\delta\rho_e(\boldsymbol{0})| > |\delta\rho_i(\boldsymbol{0})|$), although the ions are highly compressible ($|\delta\rho_i(\boldsymbol{0})| \simeq 5$) in (a), while almost incompressible ($|\delta\rho_i(\boldsymbol{0})| \simeq 0$) in (b).

A couple of notable differences exist between (a) and (b) on this charge instability: (1) the 'charge-ordering' vector $Q$ as defined by the peak position in $\delta\rho(\boldsymbol{q})$ is less than $2p_F$, the diameter of the Fermi surface of the electrons, in (a) but larger than $2p_F$ in (b); (2) the charge instability is driven by the electrons, while the ions only screen insufficiently the electronic 'charge ordering' in (a) because $|\delta\rho_e(\boldsymbol{Q})| > |\delta\rho_i(\boldsymbol{Q})|$, but it is done by the ions with partially screening electrons in (b) because $|\delta\rho_i(\boldsymbol{Q})| > |\delta\rho_e(\boldsymbol{Q})|$.

These differences imply that the charge instability for low densities has a significant influence on the electronic transport, while that for high densities does not. It is clear that the transition from liquid to solid keeps the system metallic, while it makes the translation symmetry broken; this can be understood by the fact that the charge instability for high densities is due to the localization of ions with the charge-ordering vector $\boldsymbol{Q}$, which corresponds to the reciprocal lattice

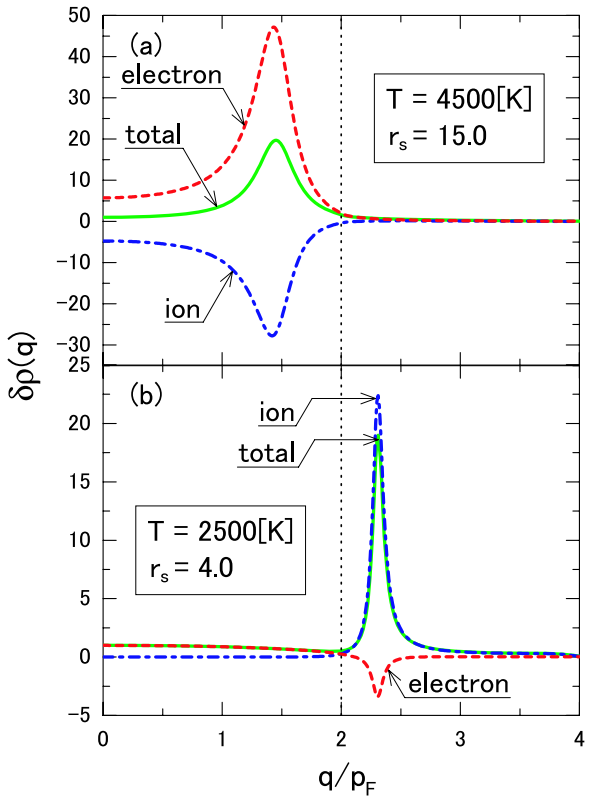


**Figure 5.** Fourier transforms of the electronic, ionic and total charge densities induced by a negative point charge at the origin, which are indicated by the broken, chain and solid curves, respectively, (a) for $T = 4500$ K and $r_s = 15.0$ and (b) for $T = 2500$ K and $r_s = 4.0$.

vector of the solid with a definite direction, and that the Fermi surface of electrons remains almost unchanged since $Q > 2p_F$. On the other hand, the charge instability for low densities is characterized by $Q < 2p_F$ and then electrons on the Fermi surface connected by $\boldsymbol{Q}$ have strong scattering amplitudes with a tendency to localization, leading at least to a decrease in the electronic conductivity. Particularly in a fluid or gaseous phase with translation symmetry (in a different manner from incommensurate-charge-density-wave formation in a solid), the entire Fermi surface may be seriously affected by $\boldsymbol{Q}$ with randomly distributed directions to preserve its rotational invariance, suggesting a new route to understanding of the metal–insulator transition.

## 6. Conclusion

We have investigated the static response functions of the fluid alkali metal by applying a perturbation method with respect to the electron–ion interaction to the first-principles Hamiltonian and found a charge instability in the dilute fluid phase above the liquid–gas critical point in the mean-field approximation based on the WCA separation. This charge instability is due to electronic density fluctuations at a finite wavevector $Q < 2p_F$, implying its intimate connection with the metal–insulator transition in fluid alkali metals.

## Acknowledgments

This work is partially supported by a Grant-in-Aid for Scientific Research in Priority Areas (No 17064004) of MEXT, Japan.

## References

[1] Mott N F 1990 *Metal–Insulator Transitions* (London: Taylor and Francis) chapter 10
[2] Hensel F 1998 *Phil. Trans. R. Soc. Lond.* A **356** 97
[3] Mott N F 1949 *Proc. Phys. Soc.* A **62** 416
[4] Landau L D and Zeldovich G 1943 *Acta Phys.-Chim. USSR* **18** 194
Landau L D and Zeldovich G 1965 *Collected Papers of L D Landau* ed D Ter Haar (Oxford: Pergamon) p 380
[5] Hansen J P and McDonald I R 2006 *Theory of Simple Liquids* (London: Elsevier) figure 1.1 in p 2
[6] Ashcroft N W and Stroud D 1978 *Solid State Phys.* **33** 1
[7] Watabe M and Hasegawa M 1973 *Properties of Liquid Metals* ed S Takeuchi (London: Taylor and Francis) p 133
[8] Moroni S, Ceperley D M and Senatore G 1995 *Phys. Rev. Lett.* **75** 689
[9] Weeks J D, Chandler D and Andersen H C 1972 *J. Chem. Phys.* **54** 5237
[10] Percus J K and Yevick G J 1958 *Phys. Rev.* **110** 1
[11] Thiele E 1963 *J. Chem. Phys.* **39** 474
[12] Wertheim M S 1963 *Phys. Rev. Lett.* **10** 321
[13] Matsuda K, Tamura K and Inui M 2007 *Phys. Rev. Lett.* **98** 096401